Self-assembly of Metallacages into Multidimensional Suprastructures with Tunable Emissions

Yan Sun,[*,†,‡,#] Yong Yao,[†,#] Heng Wang,[§] Wenxin Fu,[//] Chongyi Chen,[⊥] Manik Lal Saha,[†] Mingming Zhang,[†] Sougata Datta,[†] Zhixuan Zhou,[†] Huaxu Yu,[†] Xiaopeng Li,[§] and Peter. J. Stang[*,†]

[†] Department of Chemistry, University of Utah, 315 South 1400 East, Room 2020, Salt Lake City, Utah 84112, United States

[‡] School of Chemistry and Chemical Engineering, Yangzhou University, Yangzhou, Jiangsu 225002, PR China

[§] Department of Chemistry, University of South Florida, 4202 East Fowler Avenue, Tampa, Florida 33620, United States

[//] Beijing National Laboratory for Molecular Sciences, Institute of Chemistry, Chinese Academy of Sciences, Beijing 100190, PR China

[⊥] Ningbo Key Laboratory of Specialty Polymers, Faculty of Materials Science and Chemical Engineering, Ningbo University, Ningbo, Zhejiang 315211, PR China

# These authors contributed equally to this work.

To whom correspondence should be addressed.
Email address:
sunyan@yzu.edu.cn;
stang@chem.utah.edu

Supporting Information

1. Synthesis

2. Optical properties

3. Self-assembly of Metallacages

1. Synthesis

Synthesis of cage **1**. Tetra(4-pyridylphenyl)ethylene compound **5** (3.20 mg, 5.00 μmol, **Fig. S1**), *cis*-Pt$(PEt_3)_2(OTf)_2$ **6** (14.60 mg, 20.00 μmol, **Fig. S2-3**), and sodium sulfate-functionalized carboxylate ligand **7** (3.12 mg, 10.00 μmol, **Fig. S4**) were placed in a 2-dram vial, followed by the addition of H_2O (0.40 mL) and acetone (1.20 mL). After heating at 70 ℃ for 24 h, all the solvent was removed by a N_2 flow, and the solid was dried under vacuum. Acetone (1.00 mL) was then added to the resultant mixture, and the solution was stirred for 30 min at room temperature. Then, the mixture was filtered to remove insoluble materials. The resulting tetragonal cage **1** was precipitated with diethyl ether, isolated and dried under reduced pressure and dissolved in CD_2Cl_2 for characterization. $^{31}P\{^1H\}$ NMR (CD_2Cl_2, room temperature, 121.4 MHz) δ (ppm): 6.07 ppm (d, $^2J_{P-P}$= 19.4 Hz), -0.09 ppm (d, $^2J_{P-P}$= 19.4 Hz). The ^1H NMR spectrum of tetragonal cage **1** is shown in **Fig. S6**. ^1H NMR (CD_2Cl_2, room temperature, 400 MHz) δ (ppm): 8.66 (d, 16H), 8.36 (s, 8H), 7.97 (s, 4H), 7.68 (d, 16H), 7.17 (d, 16H), 7.15 (d, 16H).

1.1 ^1H NMR spectrum of compound 5

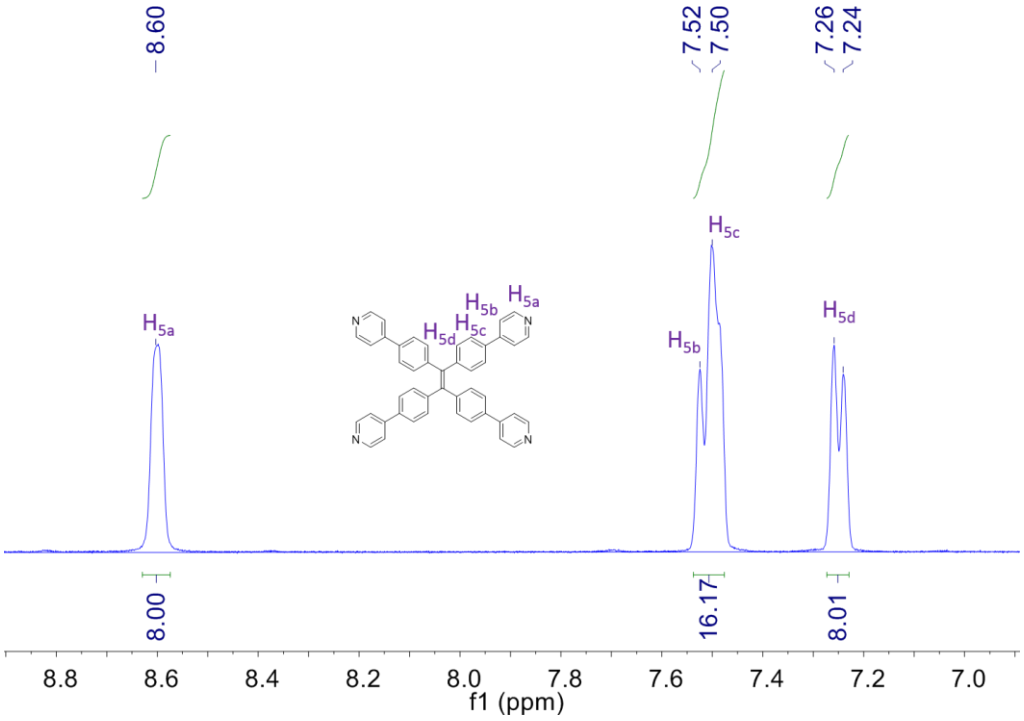

Figure S1. ^1H NMR spectrum (400 MHz, CD_2Cl_2) recorded for **5**.

1.2 ^{1}H NMR and ^{31}P {^{1}H} spectra of compound 6

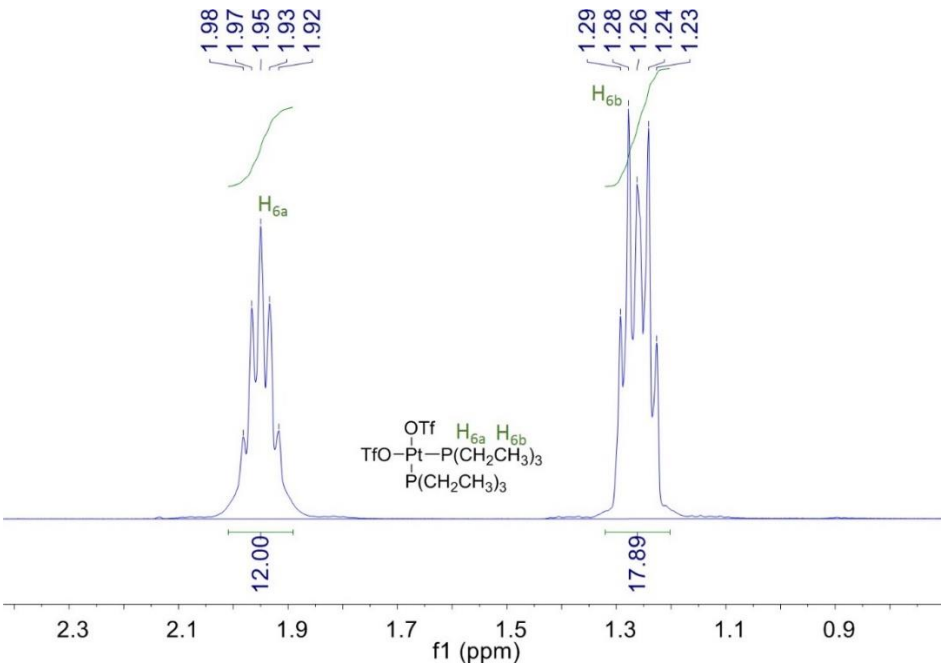

Figure S2. ^{1}H NMR spectrum (400 MHz, CD_2Cl_2) recorded for **6**.

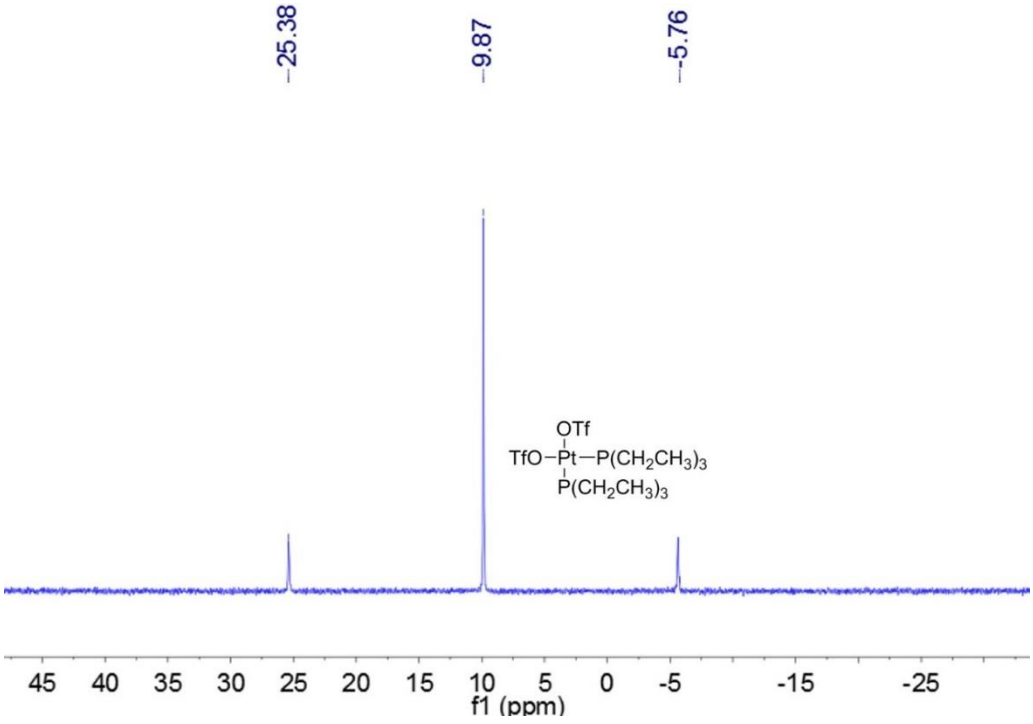

Figure S3. ^{31}P{^{1}H } NMR spectrum (300 MHz, CD_2Cl_2) recorded for **6**.

1.3 ^{1}H NMR spectrum of ligand 7

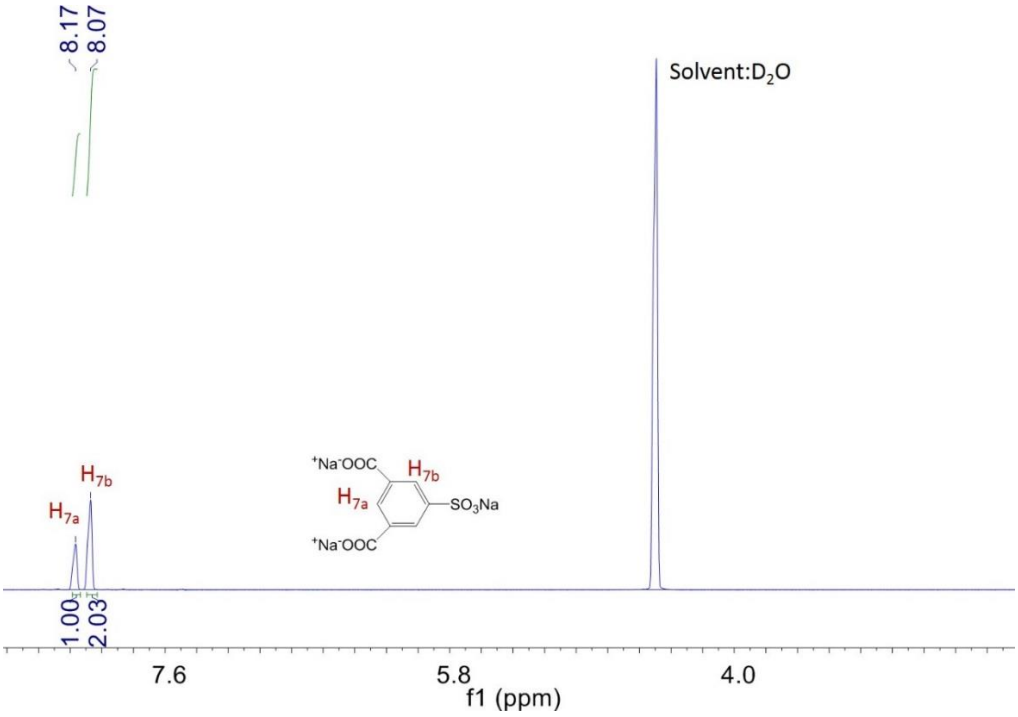

Figure S4. ^{1}H NMR spectrum (400 MHz, D_2O) recorded for ligand **7**.

1.4 ^{31}P {^{1}H} spectrum of metallacage 1

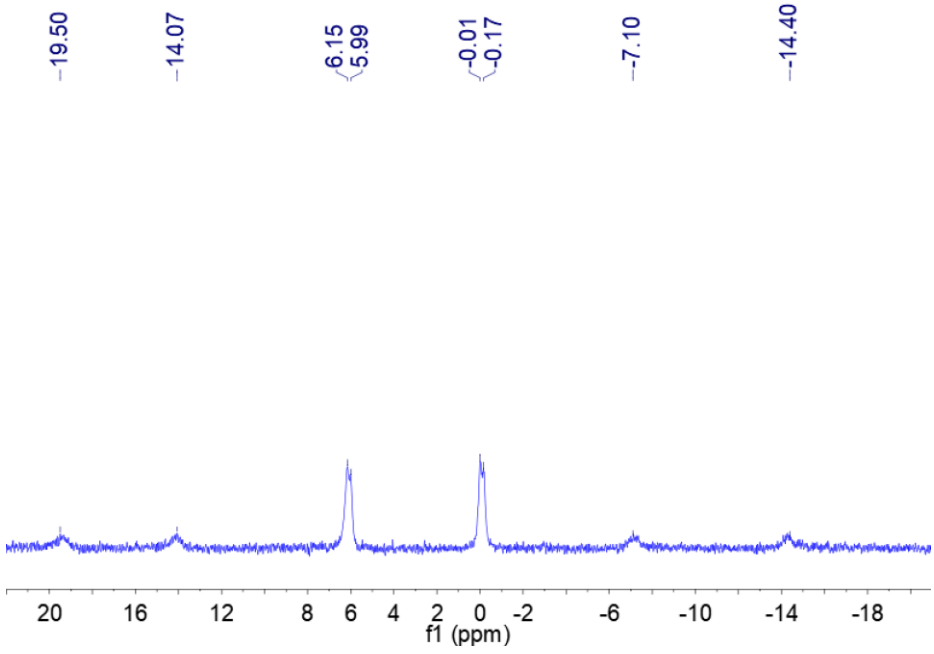

Figure S5. ^{31}P{^{1}H } NMR spectrum (CD_2Cl_2) recorded for cage **1.**

1.5 ^{1}H NMR spectrum of metallacage 1

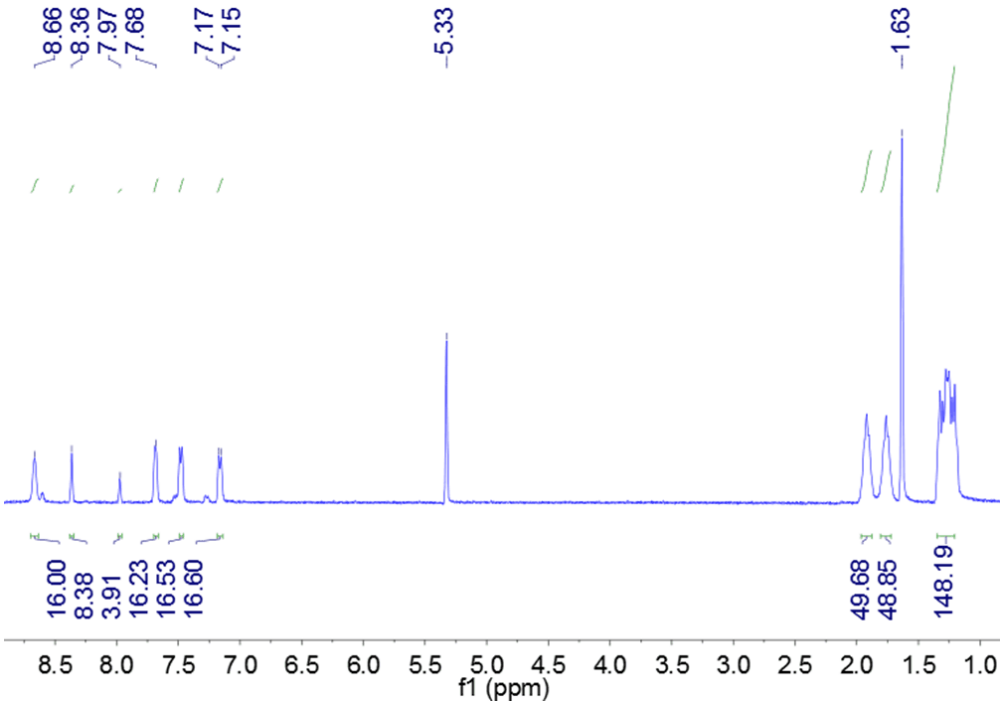

Figure S6. ^{1}H NMR spectrum (400 MHz, CD_2Cl_2) recorded for cage **1**.

Synthesis of cage **2**. Tetra(4-pyridylphenyl)ethylene compound **5** (3.20 mg, 5.00 μmol), *cis*-$Pt(PEt_3)_2(OTf)_2$ **6** (14.60 mg, 20.0 μmol), and nitro-functionalized carboxylate ligand **8** (2.60 mg, 10.0 μmol) were placed in a 2-dram vial, followed by the addition of H_2O (0.40 mL) and acetone (1.20 mL). After heating at 70 ℃ for 24 h, all the solvent was removed by a N_2 flow, and the solid was dried under vacuum. Acetone (1.00 mL) was then added to the resultant mixture, and the solution was stirred for 30 min at room temperature. Then, the mixture was filtered to remove insoluble materials. The resulting tetragonal cage **2** was precipitated with diethyl ether, isolated and dried under reduced pressure and dissolved in CD_2Cl_2 for characterization. The ^{31}P {^{1}H} NMR spectrum of tetragonal cage **2** is shown in **Fig. S7**. ^{31}P {^{1}H} NMR (CD_2Cl_2, room temperature, 121.4 MHz) δ (ppm): 5.66 ppm (d, $^{2}J_{P-P}$= 27.9 Hz), 0.44 ppm (d, $^{2}J_{P-P}$= 27.9 Hz,). The ^{1}H NMR spectrum of tetragonal cage **2** is shown in **Fig. S8**. ^{1}H NMR (CD_2Cl_2, room temperature, 400 MHz) δ (ppm): 8.65 (d, 24H), 8.39 (s, 4H), 7.71 (d, 16H), 7.50 (d, 16H), 7.19 (d, 16H). The ^{1}H NMR spectrum of ligand **8** is shown in **Fig. S9**.

1.6 $^{31}P\{^{1}H\}$ spectrum of metallacage 2

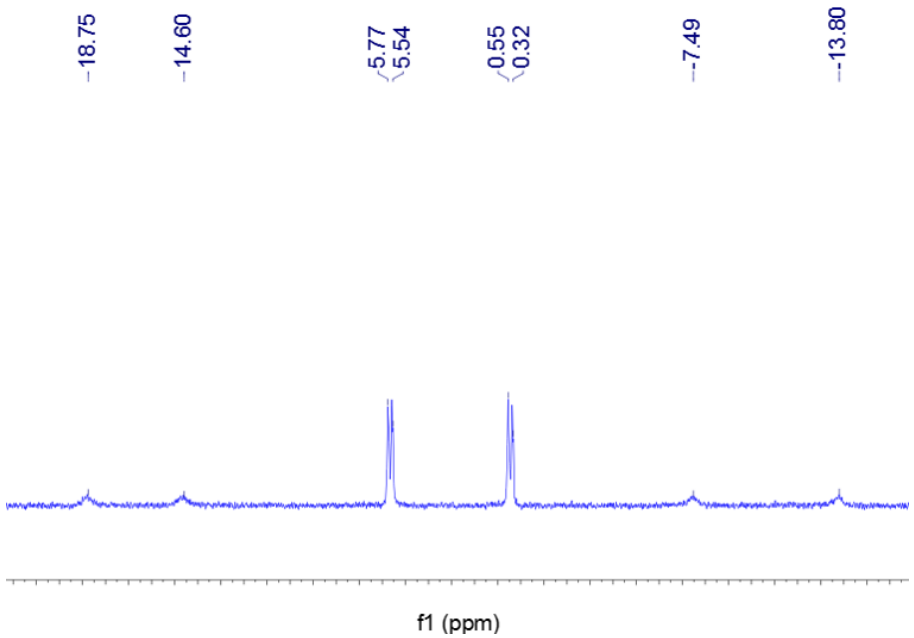

Figure S7. $^{31}P\{^{1}H\}$ NMR spectrum (CD_2Cl_2) recorded for cage **2.**

1.7 ^{1}H NMR spectrum of metallacage 2

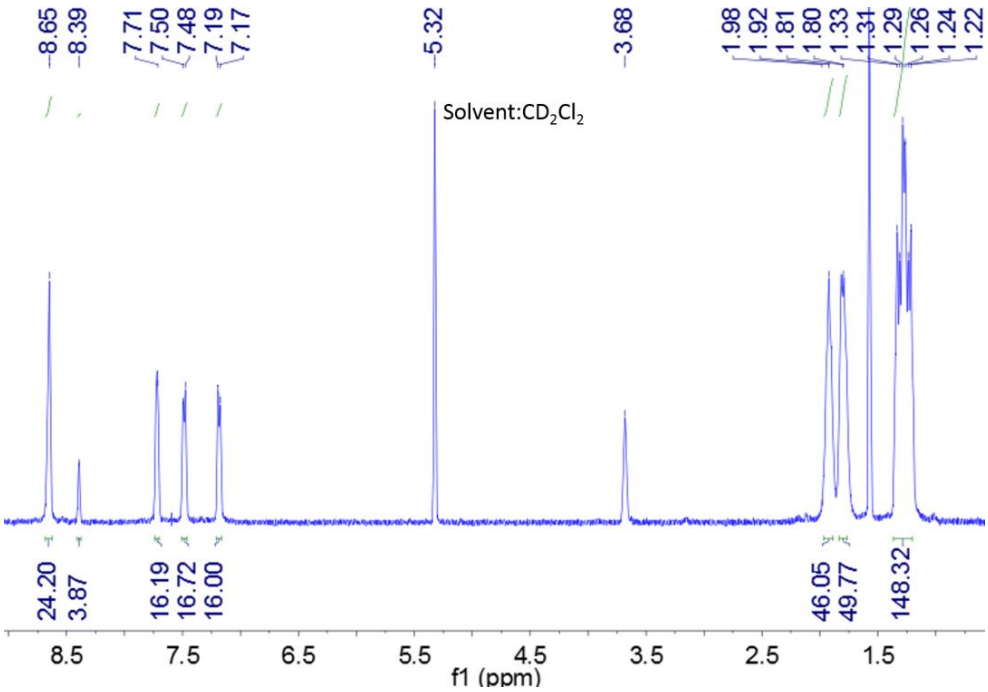

Figure S8. ^{1}H NMR spectrum (400 MHz, CD_2Cl_2) recorded for cage **2**.

1.8 ^{1}H NMR spectrum of ligand 8

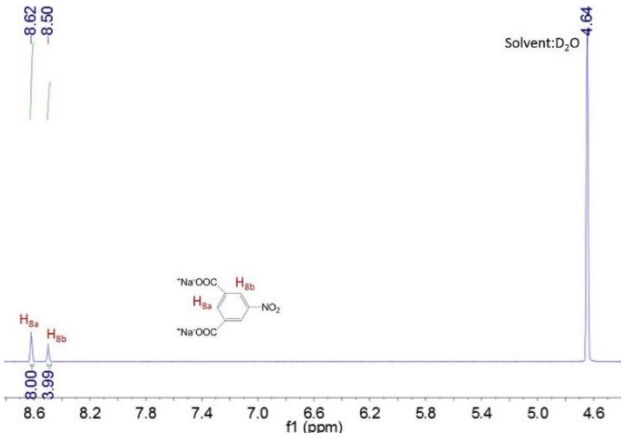

Figure S9. ^{1}H NMR spectrum (400 MHz, D_2O) recorded for ligand **8**.

Synthesis of cage **3**. Tetra(4-pyridylphenyl)ethylene compound **5** (3.20 mg, 5.00 μmol), *cis*-$Pt(PEt_3)_2(OTf)_2$ **6** (14.60 mg, 20.0 μmol), and methoxyl-functionalized carboxylate ligand **9** (2.40 mg, 10.00 μmol) were placed in a 2-dram vial, followed by the addition of H_2O (0.40 mL) and acetone (1.20 mL). After heating at 70 ℃ for 24 h, all the solvent was removed by a N_2 flow, and the solid was dried under vacuum. Acetone (1.00 mL) was then added to the resultant mixture, and the solution was stirred for 30 min at room temperature. Then, the mixture was filtered to remove insoluble materials. The resulting tetragonal cage **3** was precipitated with diethyl ether, isolated and dried under reduced pressure and dissolved in CD_2Cl_2 for characterization. The ^{31}P {^{1}H} NMR spectrum of tetragonal cage **3** is shown in **Fig. S10**. ^{31}P {^{1}H} NMR (CD_2Cl_2, room temperature, 121.4 MHz) δ (ppm): 6.14 ppm (d, $^{2}J_{P-P}$= 21.8 Hz), 0.52 ppm (d, $^{2}J_{P-P}$= 21.8 Hz). The ^{1}H NMR spectrum of tetragonal cage **3** is shown in **Fig. S11**. ^{1}H NMR (CD_2Cl_2, room temperature, 400 MHz) δ (ppm): 8.67 (d, 16H), 7.65 (d, 16H), 7.51 (s, 4H), 7.45 (d, 16H), 7.20 (s, 8H), 7.18 (d, 16H), 3.82 (s, 12H). The ^{1}H NMR spectrum of ligand **9** is shown in **Fig. S12**. The ^{31}P{^{1}H} spectrum of cage **3** show two doublets of approximately equal intensity with concomitant ^{195}Pt satellite peaks corresponding to two distinct phosphorous environments (**Fig.1e**, **Fig. S10**). In the ^{1}H NMR spectrum of cage **3** (**Fig. 1j**, **Fig. S11**), the protons of the pyridyl groups are shifted downfield ($\Delta\delta[H_{5a}]$ = 0.07 ppm; $\Delta\delta[H_{5b}]$ = 0.13 ppm) relative to those of ligand **5**, consistent with the coordination of the N atoms to the platinum centers. The protons corresponding to dicarboxylate ligand **9** are observed at δ = 7.51 and 7.45 ppm (**Fig. S12**).

1.9 $^{31}P\{^{1}H\}$ spectrum of metallacage 3

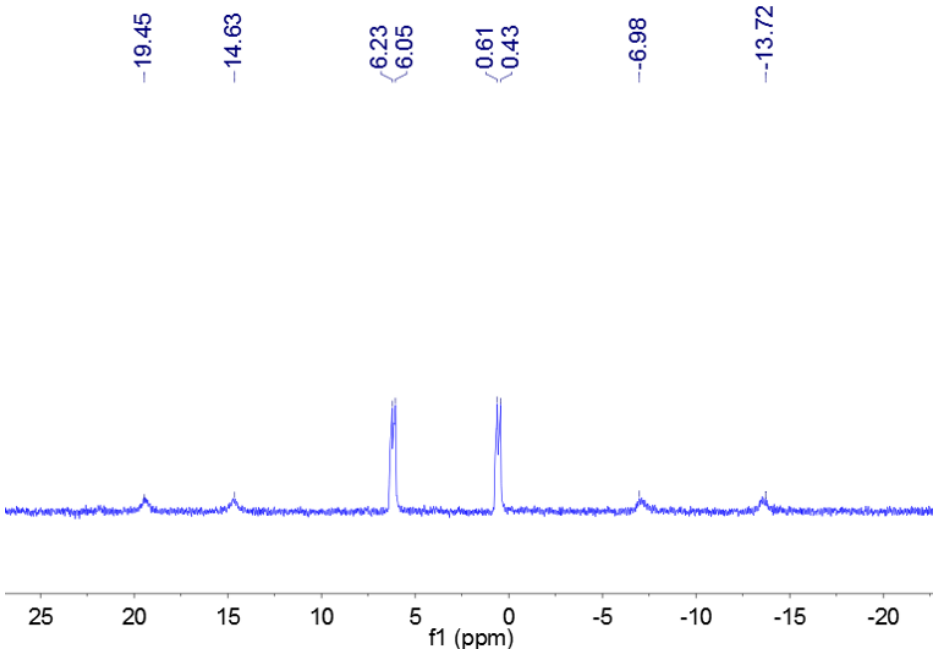

Figure S10. $^{31}P\{^{1}H\}$ NMR spectrum (CD_2Cl_2) recorded for cage **3.**

1.10 ^{1}H NMR spectrum of metallacage 3

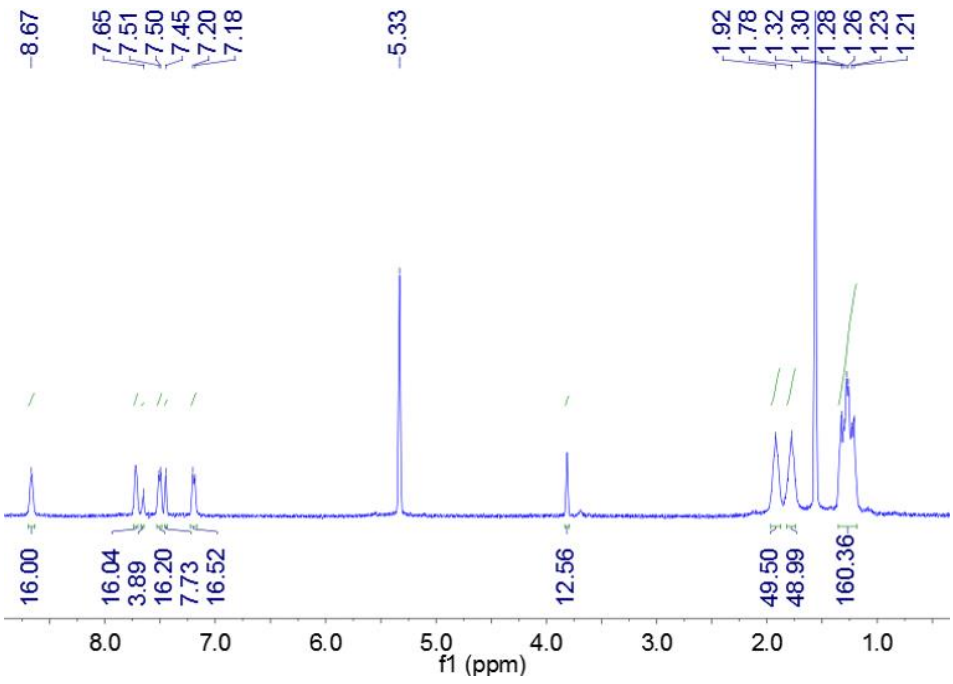

Figure S11. ^{1}H NMR spectrum (400 MHz, CD_2Cl_2,) recorded for cage **3**.

1.11 ^{1}H NMR spectrum of ligand 9

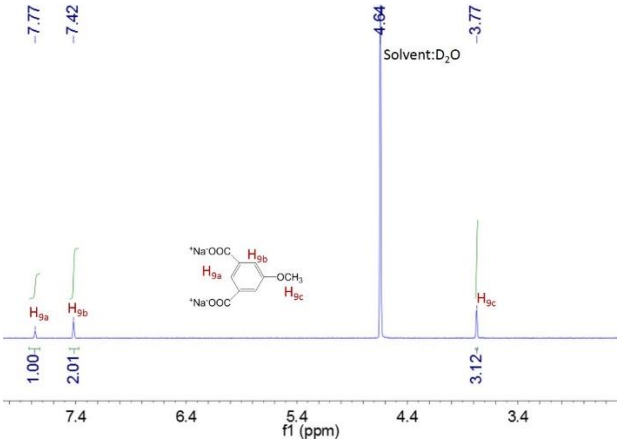

Figure S12. ^{1}H NMR spectrum (400 MHz, D_2O) recorded for ligand **9**.

Synthesis of cage **4**. Tetra(4-pyridylphenyl)ethylene compound **5** (3.20 mg, 5.00 μmol), *cis*-$Pt(PEt_3)_2(OTf)_2$ **6** (14.60 mg, 20.0 μmol), and amine-functionalized carboxylate ligand **10** (2.25 mg, 10.00 μmol) were placed in a 2-dram vial, followed by the addition of H_2O (0.40 mL) and acetone (1.20 mL). After heating at 70 ℃ for 24 h, all the solvent was removed by a N_2 flow, and the solid was dried under vacuum. Acetone (1.00 mL) was then added to the resultant mixture, and the solution was stirred for 30 min at room temperature. Then, the mixture was filtered to remove insoluble materials. The resulting tetragonal cage **4** was precipitated with diethyl ether, isolated and dried under reduced pressure and dissolved in CD_2Cl_2 for characterization. The ^{31}P {^{1}H} NMR spectrum of tetragonal cage **4** is shown in **Fig. S13**. ^{31}P {^{1}H} NMR (CD_2Cl_2, room temperature, 121.4 MHz) δ (ppm): 6.38 ppm (d, $^{2}J_{P-P}$= 20.6 Hz), 0.30 ppm (d, $^{2}J_{P-P}$= 20.6 Hz). The ^{1}H NMR spectrum of tetragonal cage **4** is shown in **Fig. S14**. ^{1}H NMR (CD_2Cl_2, room temperature, 400 MHz) δ (ppm): 8.67 (d, 16H), 7.71 (d, 16H), 7.50 (d, 16H), 7.37 (s, 4H), 7.24 (s, 8H), 7.19 (d, 16H). The ^{1}H NMR spectrum of ligand **10** is shown in **Fig. S15**. The ^{31}P{^{1}H} spectrum of cage **4** show two doublets of approximately equal intensity with concomitant ^{195}Pt satellite peaks corresponding to two distinct phosphorous environments (**Fig. 1f**, **Fig. S13**). In the ^{1}H NMR spectrum of cage **4** (**Fig. 1k**, **Fig. S14**), the protons of the pyridyl groups are shifted downfield ($\Delta\delta[H_{5a}]$ = 0.07 ppm; $\Delta\delta[H_{5b}]$ = 0.19 ppm) relative to those of ligand **5**, consistent with the coordination of the N atoms to the platinum centers. The protons corresponding to dicarboxylate ligand **10** are observed at δ = 7.37 and 7.24 ppm (**Fig. 1k**, **Fig. S15**). The well-defined signals in both the ^{31}P{^{1}H} and ^{1}H NMR spectra indicate a discrete structure was the sole assembly product.

1.12 $^{31}P\{^{1}H\}$ spectrum of metallacage 4

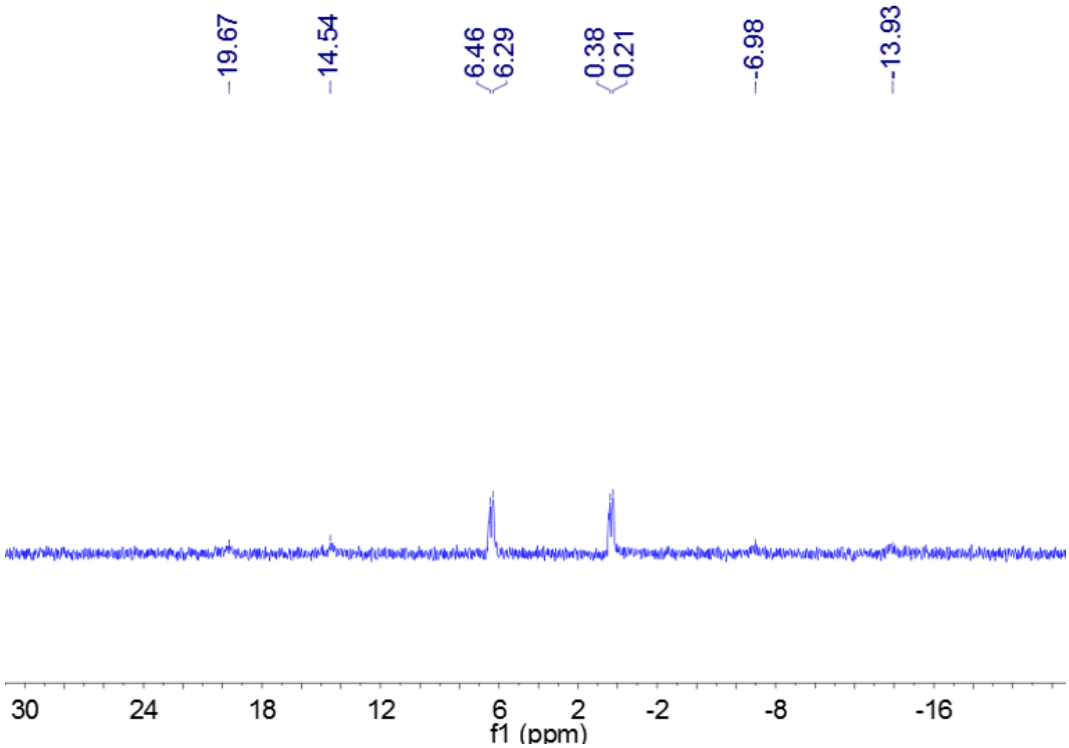

Figure S13. $^{31}P\{^{1}H\}$ NMR spectrum (CD_2Cl_2) recorded for cage **4.**

1.13 ^{1}H NMR spectrum of metallacage 4

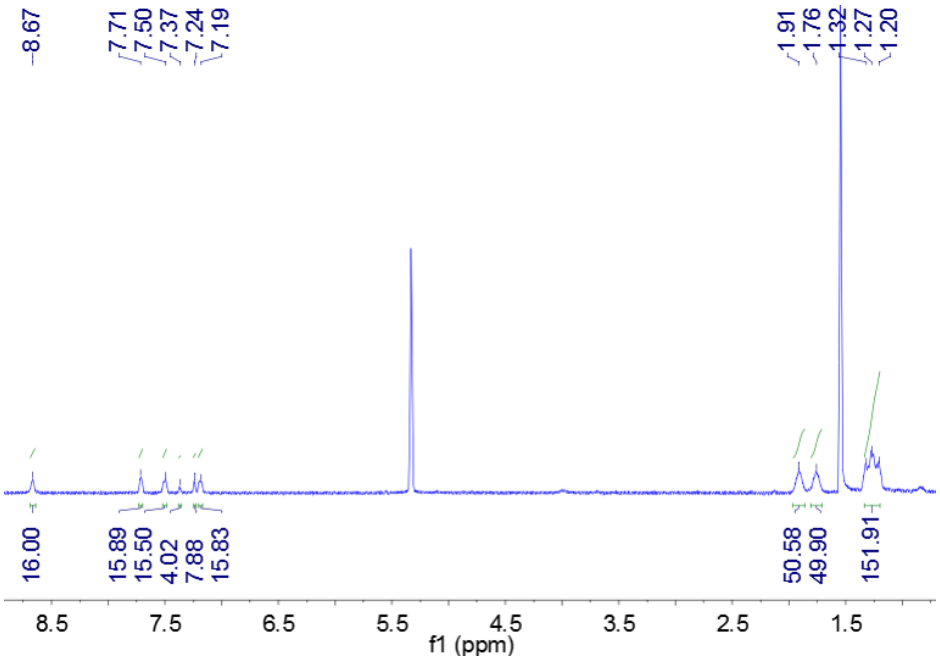

Figure S14. ^{1}H NMR spectrum (400 MHz, CD_2Cl_2) recorded for cage **4**.

1.14 ^{1}H NMR spectrum of ligand 10

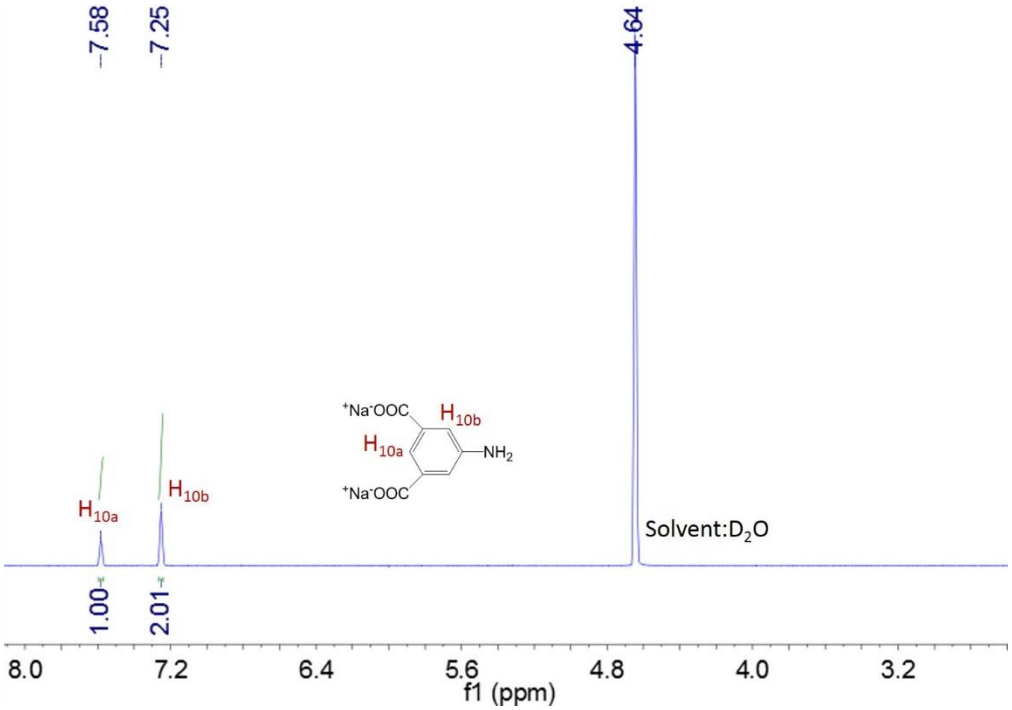

Figure S15. ^{1}H NMR spectrum (400 MHz, D_2O) recorded for ligand **10**.

1.15 ESI -TOF-MS spectrum of metallacage 1

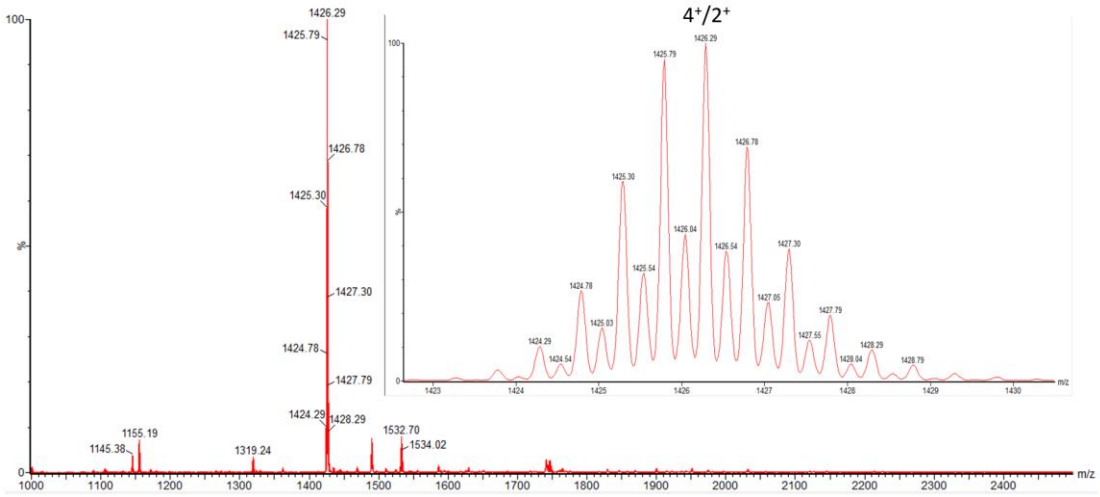

Figure S16. ESI -TOF-MS spectrum of cage **1**.

1.16 ESI -TOF-MS spectrum of metallacage 2

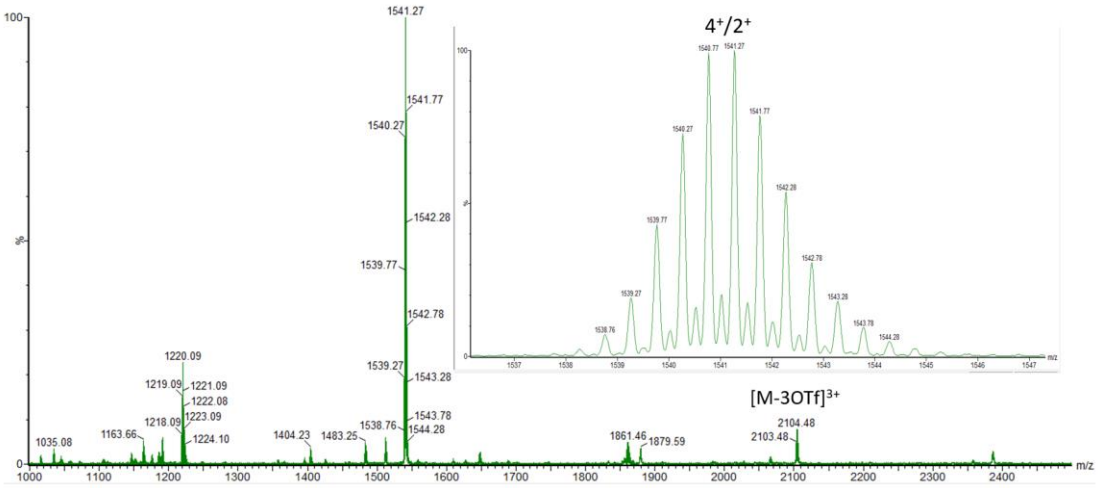

Figure S17. ESI –TOF-MS spectrum of cage **2.**

1.17 ESI -TOF-MS spectrum of metallacage 3

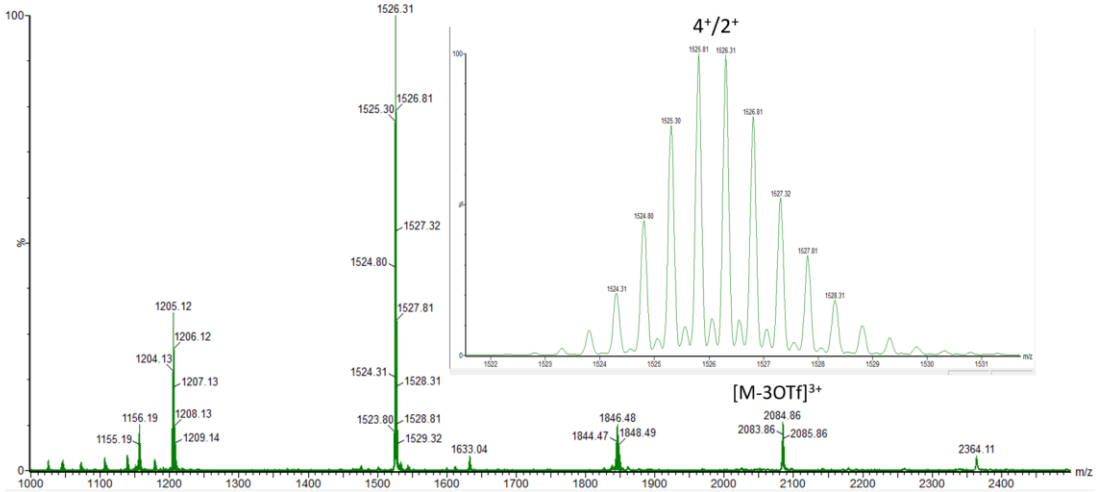

Figure S18. ESI –TOF-MS spectrum of cage **3.**

1.18 ESI -TOF-MS spectrum of metallacage 4

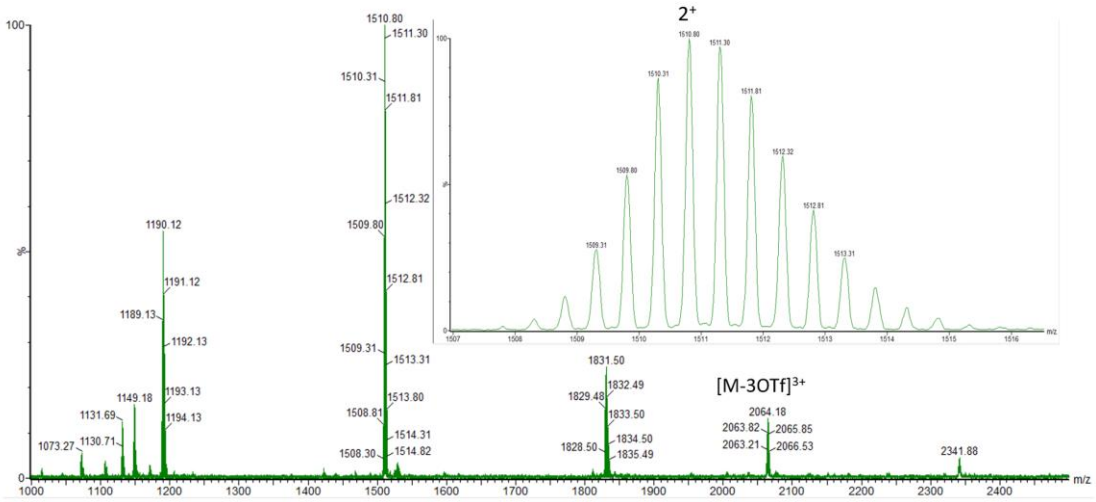

Figure S19 ESI –TOF-MS spectrum of cage **4.**

2. Optical properties

2.1 UV-Vis spectra of the four cages in different solvents

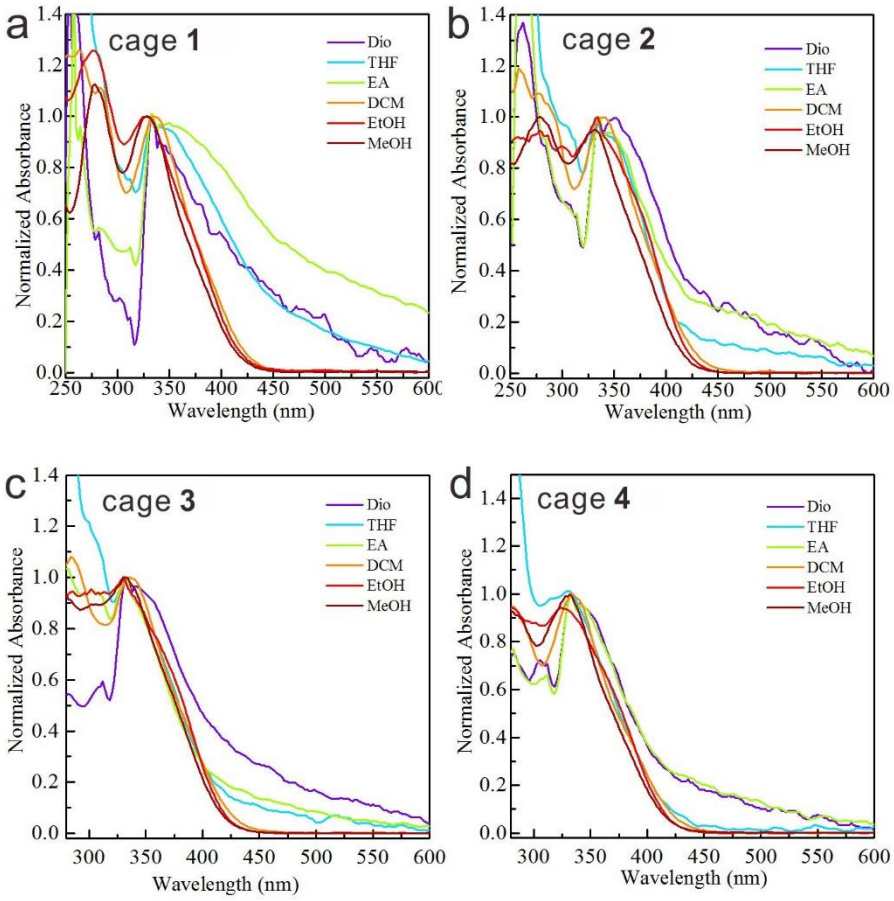

Figure S20. UV-Vis spectra of the four cages in different solvents (c = 25.0 μM).

2.2 Fluorescence spectra of the four cages in different solvents

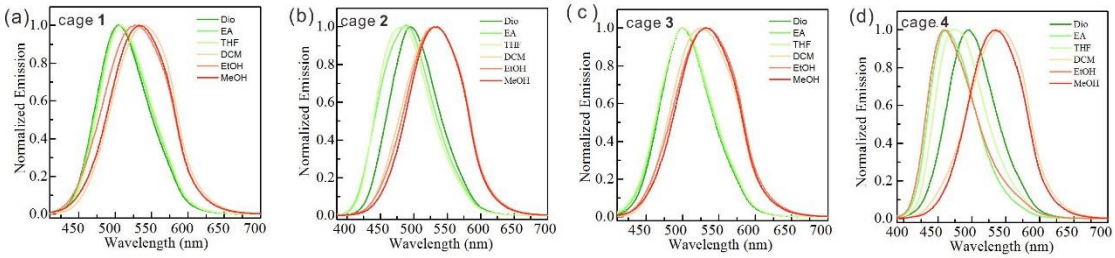

Figure S21. Fluorescence spectra of the four cages in different solvents. (λ_{ex} = 365 nm, c = 25.0 μM).

2.3 ^{31}P{^{1}H} NMR spectra of the four metallacages in dichloromethane

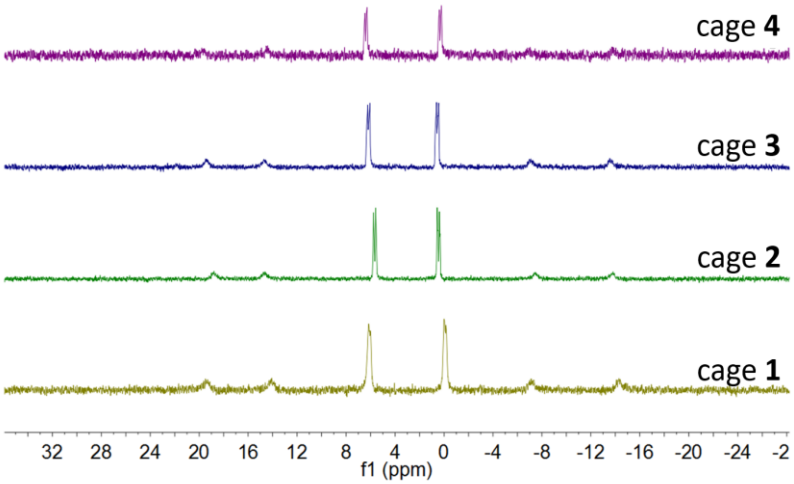

Figure S22. ^{31}P{^{1}H} NMR spectra of the four metallacages in dichloromethane.

2.4 ^{31}P{^{1}H} NMR spectra of the four metallacages in methanol

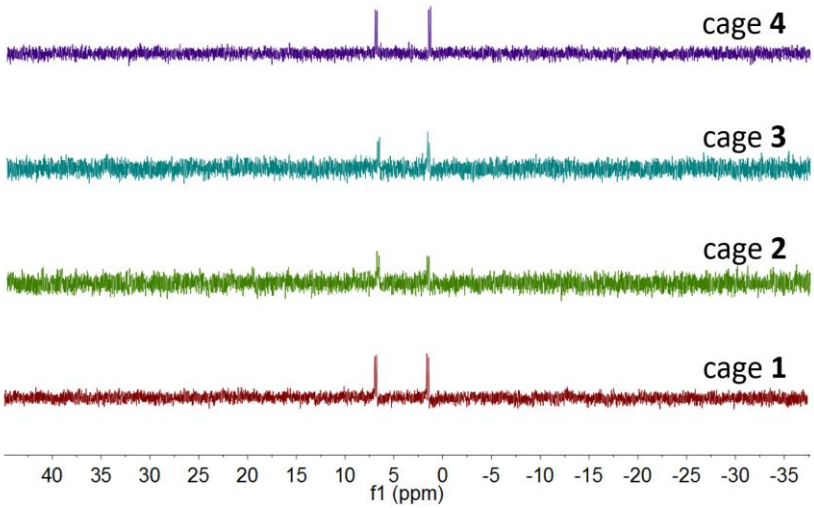

Figure S23. ^{31}P{^{1}H} NMR spectra of the four metallacages in methanol.

2.5 ^{31}P{^{1}H} NMR spectra of the two metallacages in ethanol

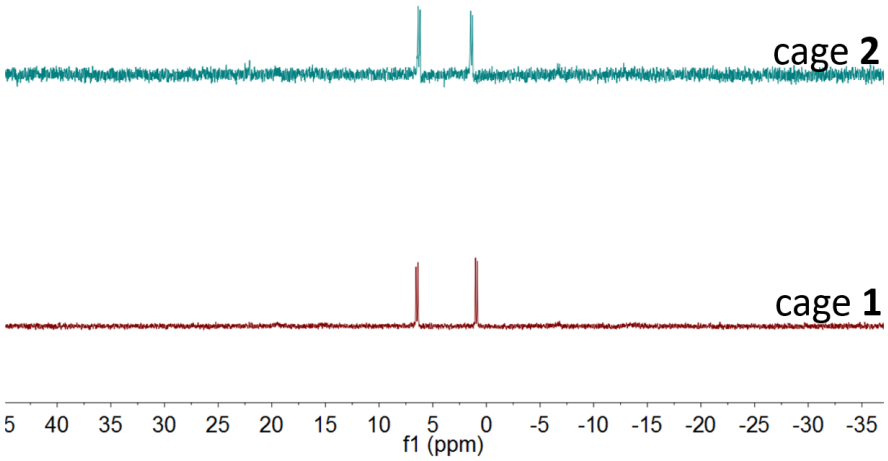

Figure S24. ^{31}P{^{1}H} NMR spectra of the two metallacages in ethanol

2.6 Fluorescence spectra of TPE in dioxane, ethyl acetate, and tetrahydrofuran

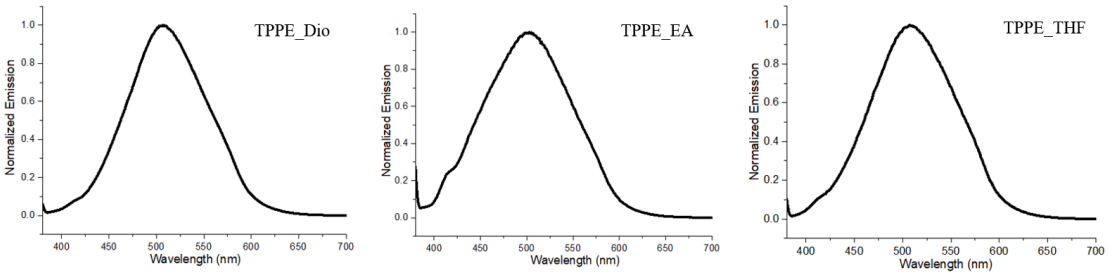

Figure S25. Fluoresence spectra of TPE in dioxane (Dio), ethyl acetate (EA), and tetrahydrofuran (THF).

3. Self-assembly of Metallacages

3.1 Fluorescence spectrum of cage 1 in water

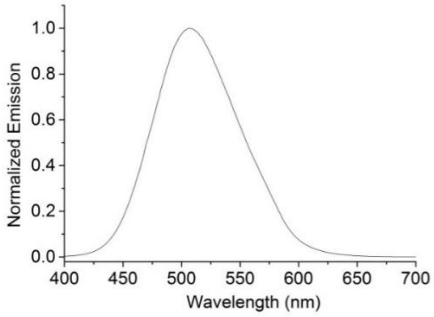

Figure S26. Fluorescence spectrum of cage **1** in water.

3.2 Scheme of the self-assembly of cage 1

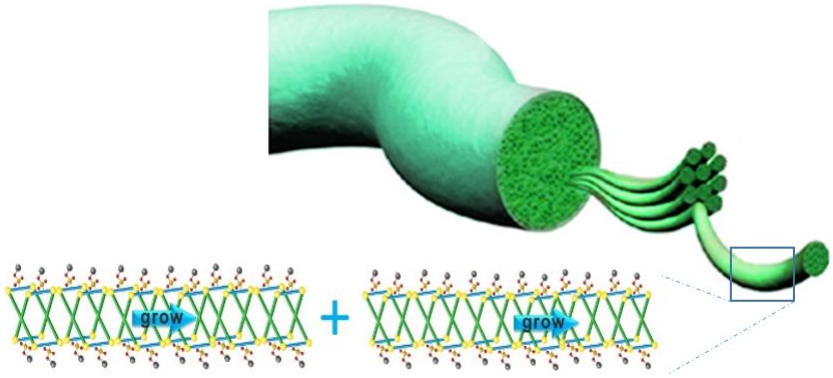

Figure S27. Scheme of the self-assembly of cage **1** in water (the illustrations are not drawn to scale).

3.3 Fluorescence spectrum of cage 2 in tetrahydrofuran

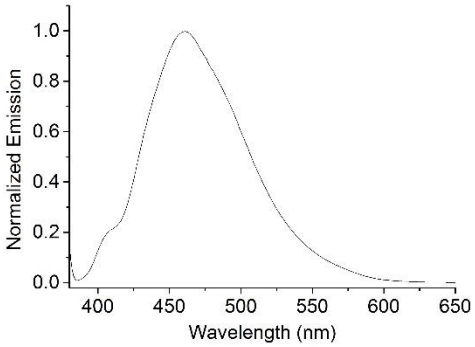

Figure S28. Fluorescence spectrum of cage **2** in tetrahydrofuran.

3.4 Scheme of cage 2-based microplates

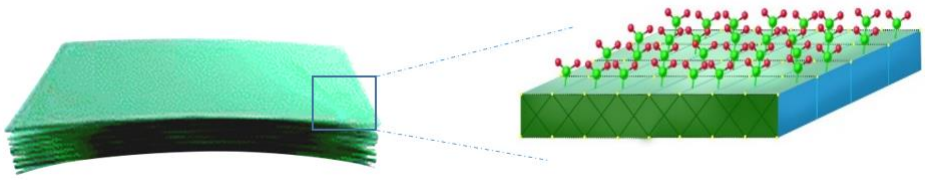

Figure S29. Scheme of the self-assembly of cage **2** in tetrahydrofuran (the illustrations are not drawn to scale).

3.5 Cage 2-based microfilm

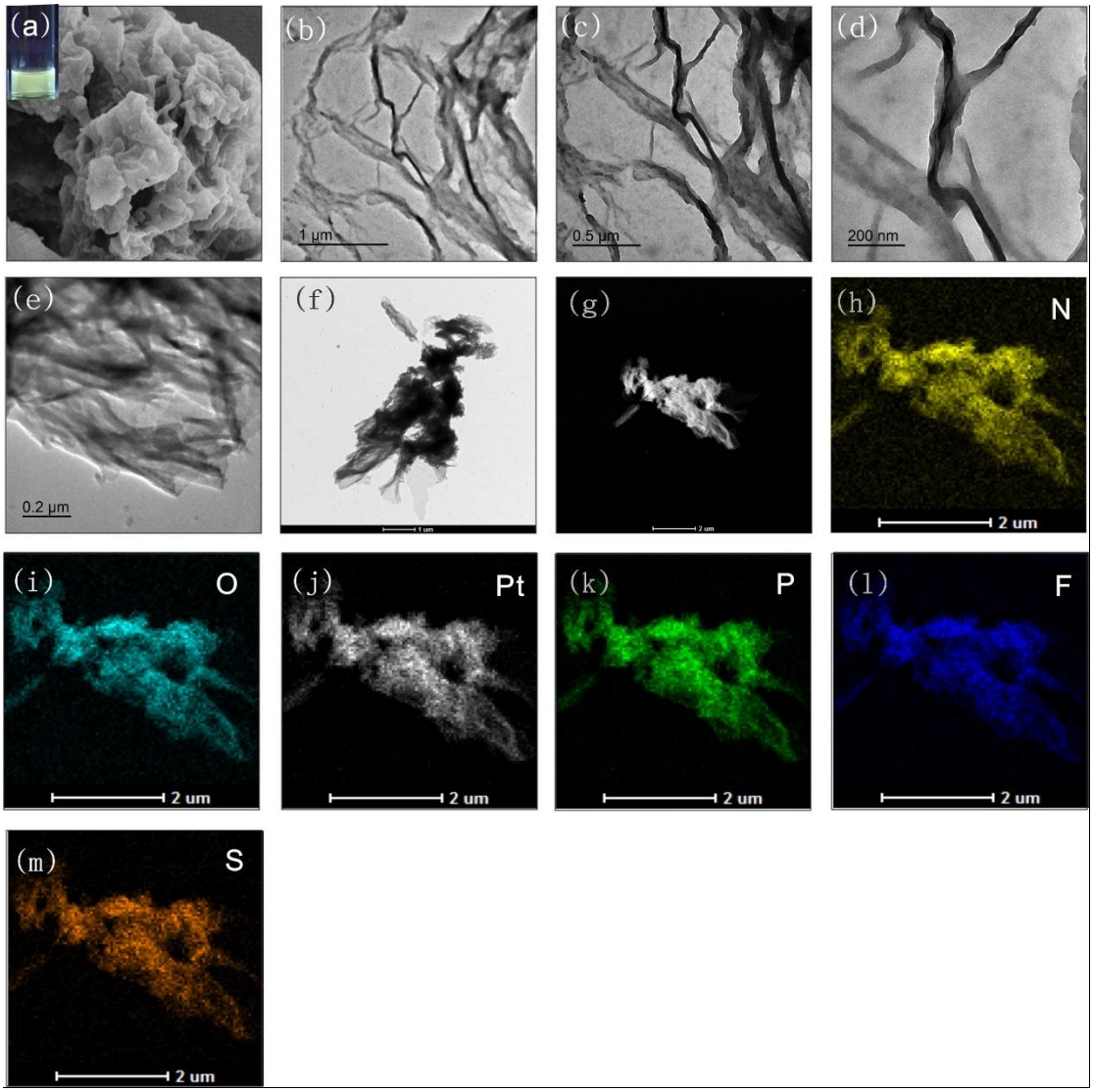

Figure S30. (a) SEM image of the cage **2**-based microfilm (inset: digital photo of the cage **2** solution); (b-e) TEM images of the microfilm at different magnifications; (f-g) TEM and STEM images of the microfilm. EDX mapping images of the cage **2**-based microfilm: the elemental distributions of (h) N, (i) O, (j) Pt, (k) P, (l) F, and (m) S.

3.6 Fluorescence spectrum of cage 2

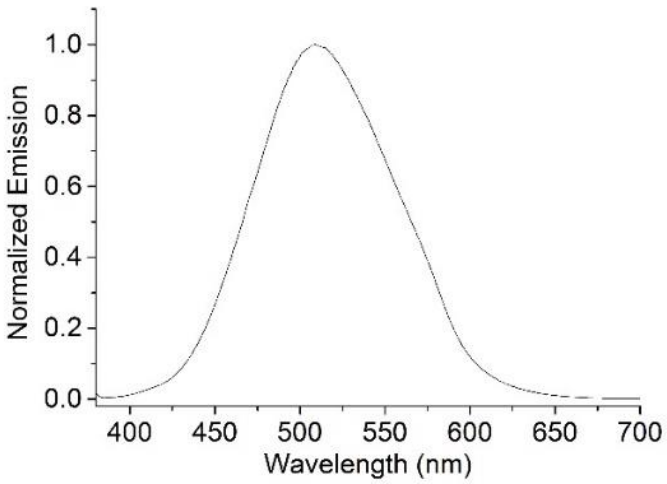

Figure S31. Fluorescence spectrum of cage **2** in ethanol.

3.7 Cage 4-based microleaves

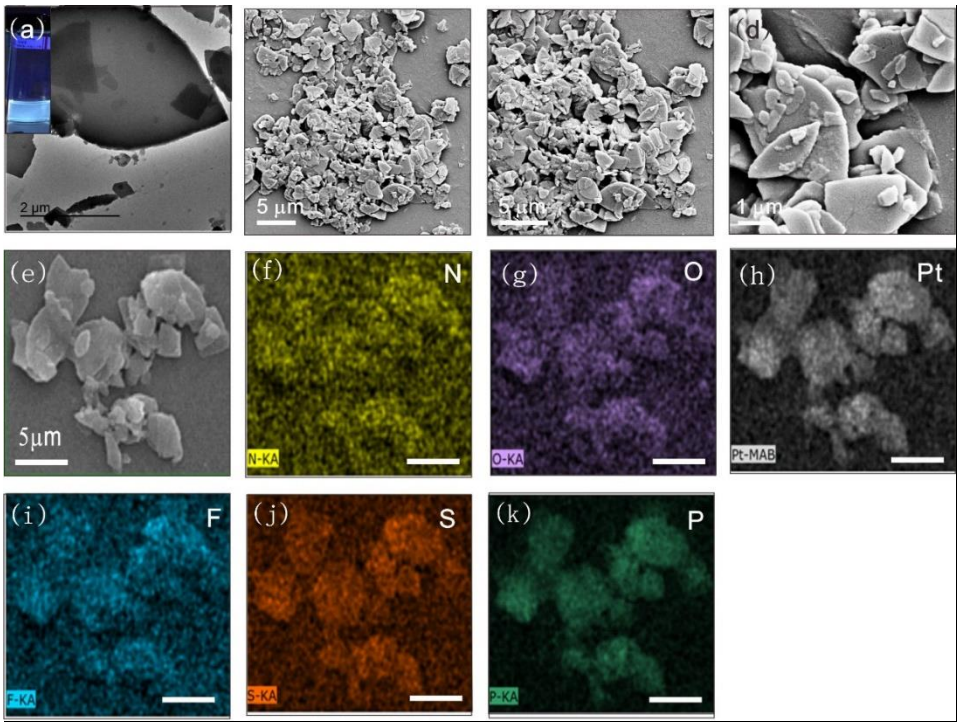

Figure S32. (a) TEM image of the cage **4**-based micro-leaves (inset: digital photo of the cage **4** solution); (b-e) SEM images of the cage **4**-based micro-leaves in tetrahydrofuran at different magnifications; corresponding EDX mapping images of the cage **4**-based micro-leaves: the elemental distributions of (f) N, (g) O, (h) Pt, (i) F, (j) S, and (k) P (scale bar: 5μm).

3.8 Fluorescence spectrum of cage 4

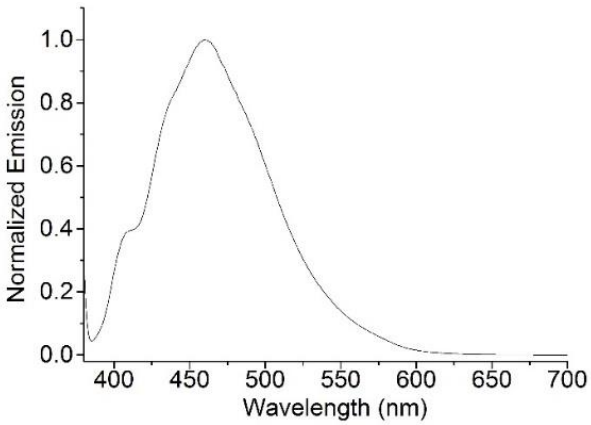

Figure S33. Fluorescence spectrum of cage **4** in tetrahydrofuran.

3.9 Fluorescence spectrum of cage 3

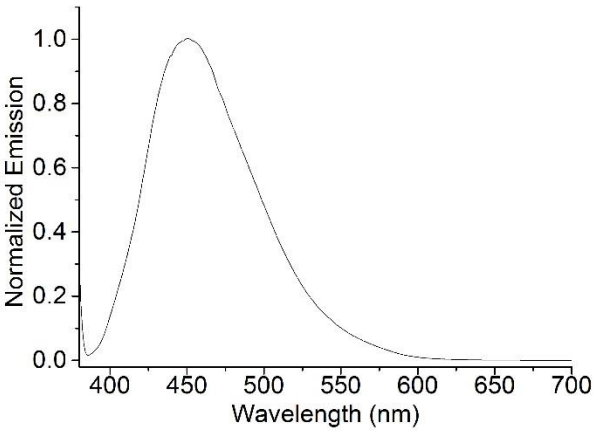

Figure S34. Fluorescence spectrum of cage **3** in tetrahydrofuran.

3.10 Scheme of the self-assembly of cage 3

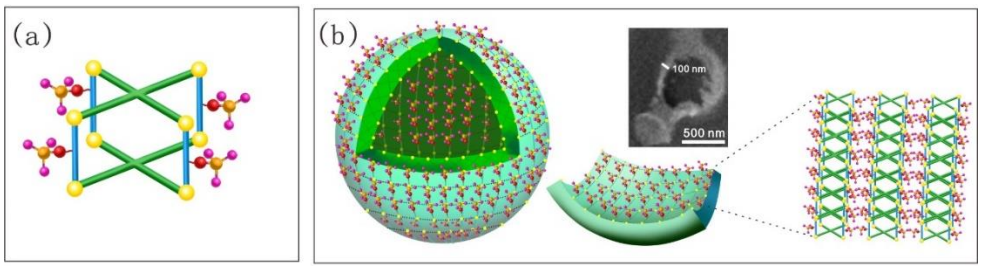

Figure S35. (a) A diagrammatic sketch of cage **3**; (b) scheme of the self-assembly of cage **3** in tetrahydrofuran (inset: SEM image of hollow sphere).

3.11 Fluorescence spectrum of cage 1 in ethanol

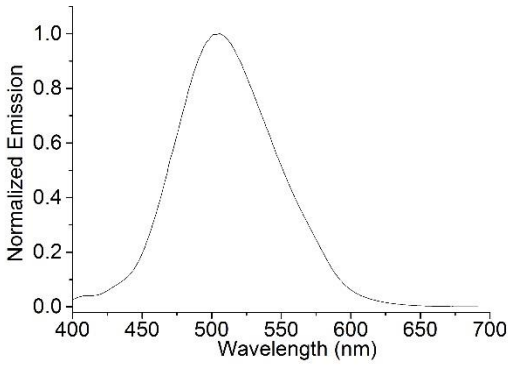

Figure S36. Fluorescence spectrum of cage **1** in ethanol.

3.12 Cage 1-based microspheres in ethanol

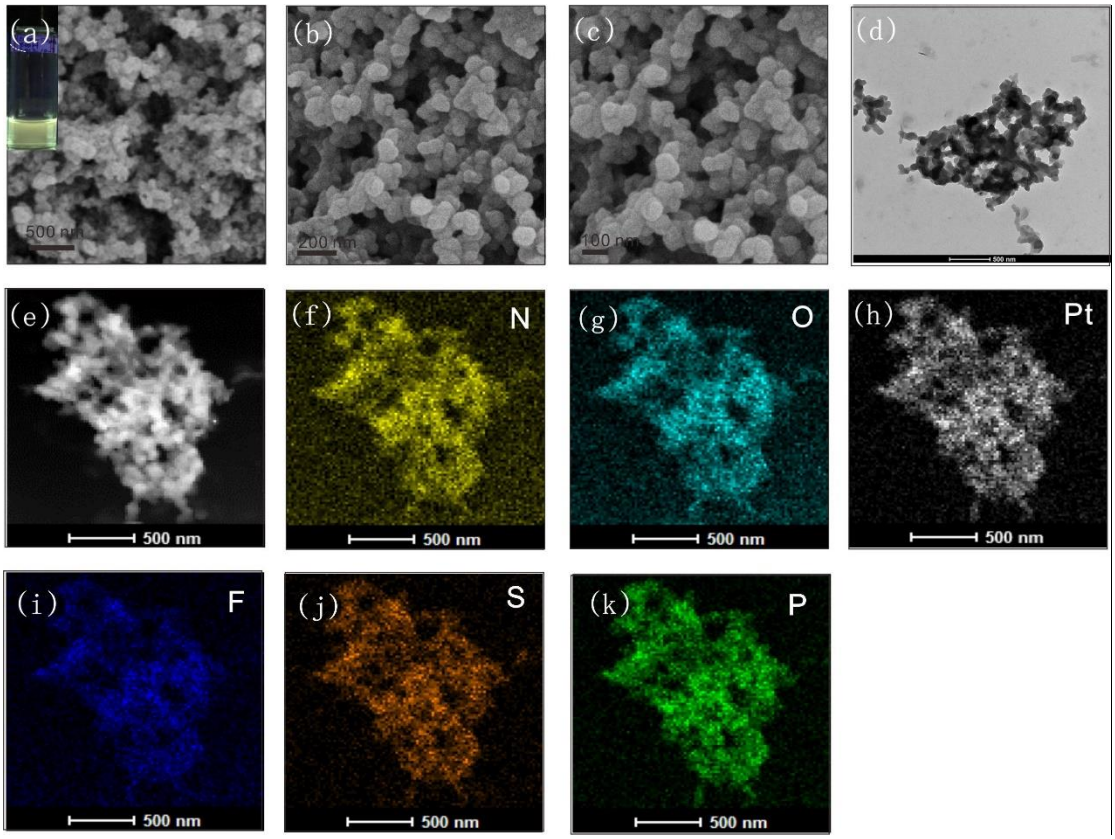

Figure S37. (a) SEM images of the cage **1**-based microspheres in ethanol; (b-c) SEM images of microspheres at different magnifications; (d) TEM image of the microspheres (scale bar: 500 nm); (e) STEM image of the microspheres; corresponding EDX mapping images of the cage **1** based microspheres: the elemental distributions of (f) N, (g) O, (h) Pt, (i) F, (j) S, and (k) P.

3.13 Fluorescence spectrum of cage 3 in tetrahydrofuran

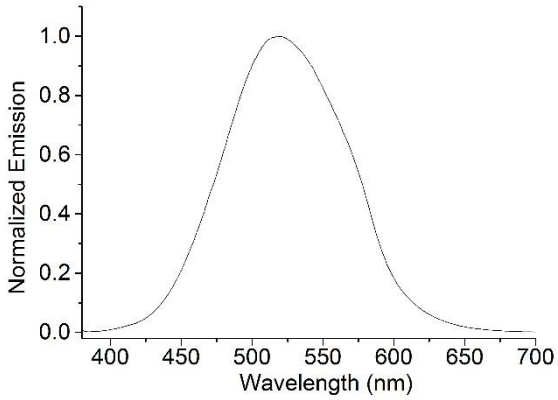

Figure S38. Fluorescence spectrum of cage **1** in tetrahydrofuran.

3.14 Cage 1-based microspheres in tetrahydrofuran

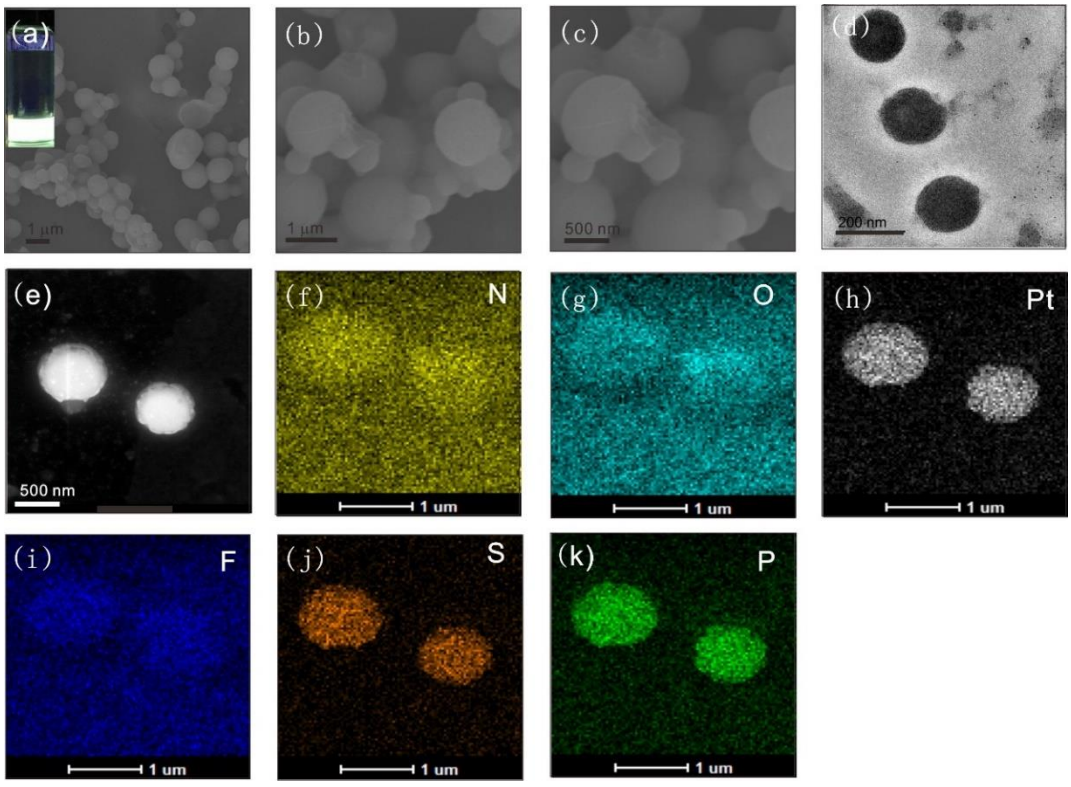

Figure S39. (a) SEM images of the cage **1**-based microspheres in tetrahydrofuran (inset: digital photo of the **cage 1** in tetrahydrofuran); (b-c) SEM images of microspheres at different magnifications; (d) TEM image of the microspheres; (e) STEM image of the microspheres; EDX mapping images of the cage **1**-based microspheres: the elemental distributions of (f) N, (g) O, (h) Pt, (i) F, (j) S, and (k) P.

3.15 ^{31}P{^{1}H} NMR spectra of the cage 1 in ethanol for seven days

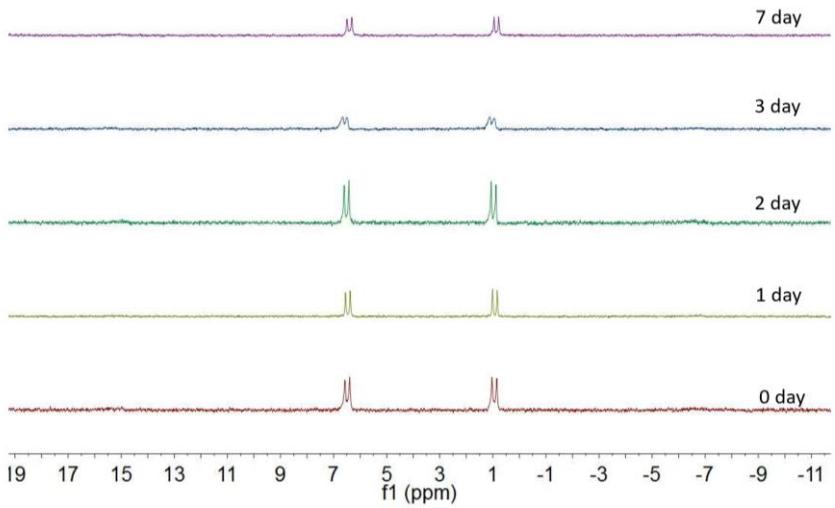

Figure S40. Partial ^{31}P{^{1}H} NMR spectra of cage **1** in ethanol for seven days.

3.16 ^{31}P{^{1}H} NMR spectra of the cage 2 in ethanol for seven days

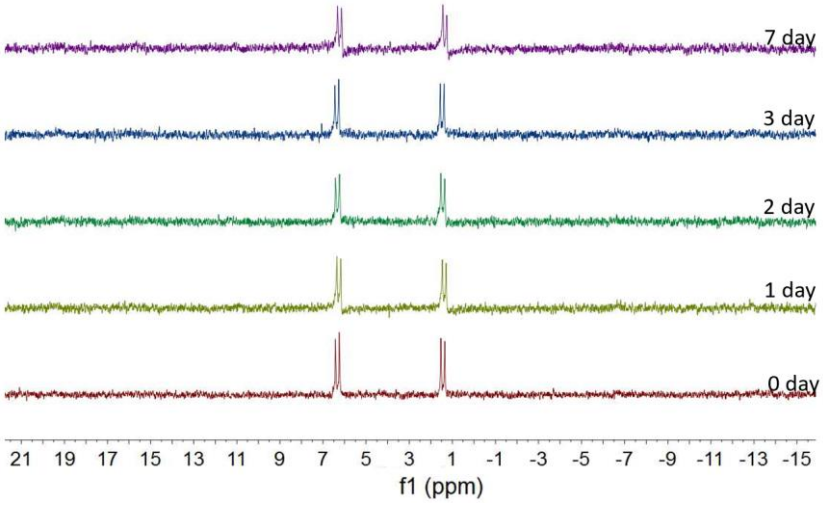

Figure S41. Partial ^{31}P{^{1}H} NMR spectra of cage **2** in ethanol for seven days.

3.17 ^{31}P{^{1}H} NMR spectra of the cage 1 in water for seven days

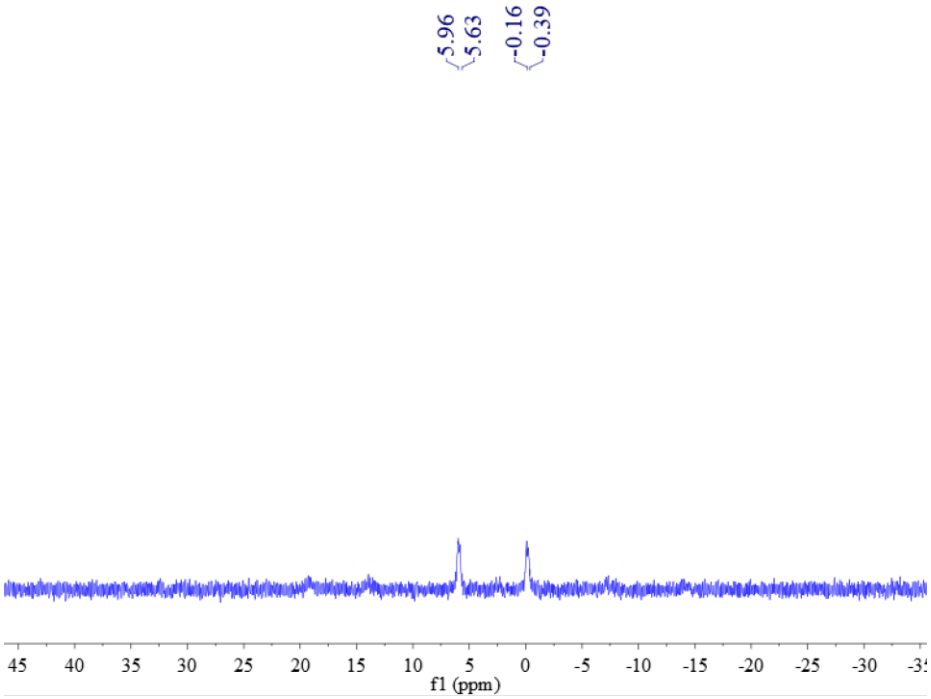

Figure S42. ^{31}P{^{1}H} NMR spectra of cage **1** based aggregates formed in water for seven days (resuspended in DCM).

3.18 ^{31}P{^{1}H} NMR spectra of the cage 1 in THF for seven days

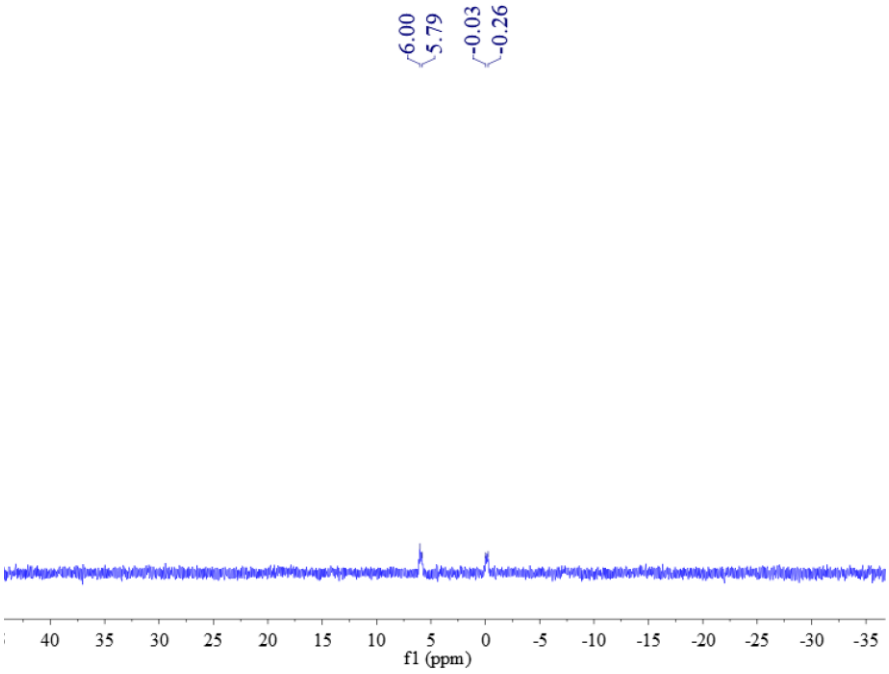

Figure S43. ^{31}P{^{1}H} NMR spectra of cage **1** based aggregates formed in THF for seven days (resuspended in DCM).

3.19 ^{31}P{^{1}H} NMR spectra of the cage 2 in THF for seven days

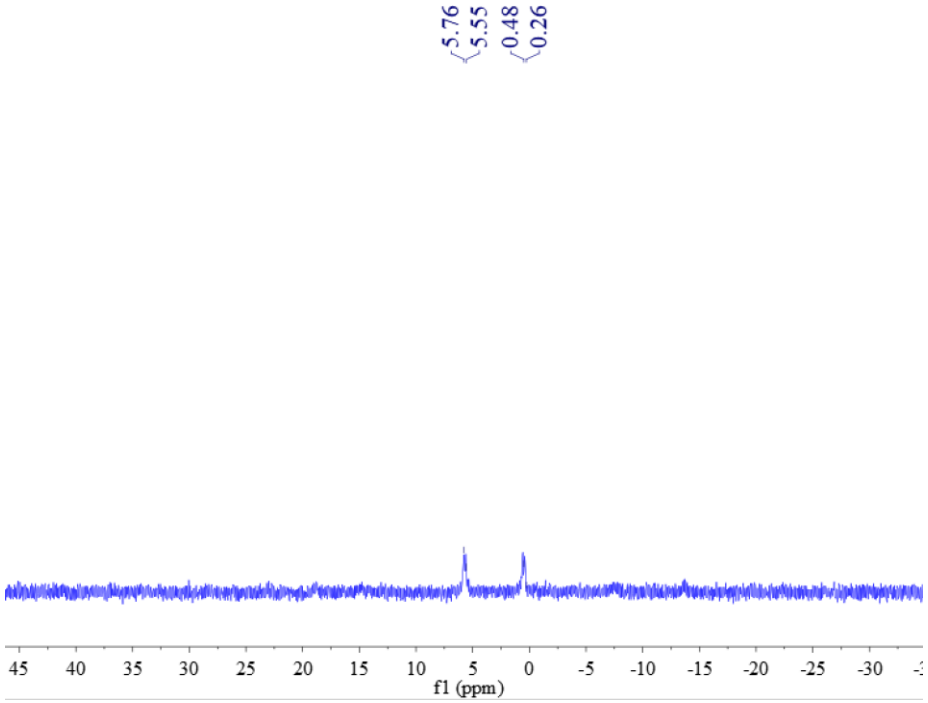

Figure S44. ^{31}P{^{1}H} NMR spectra of cage **2** based aggregates formed in THF for seven days (resuspended in DCM).

3.20 ^{31}P{^{1}H} NMR spectra of the cage 3 in THF for seven days

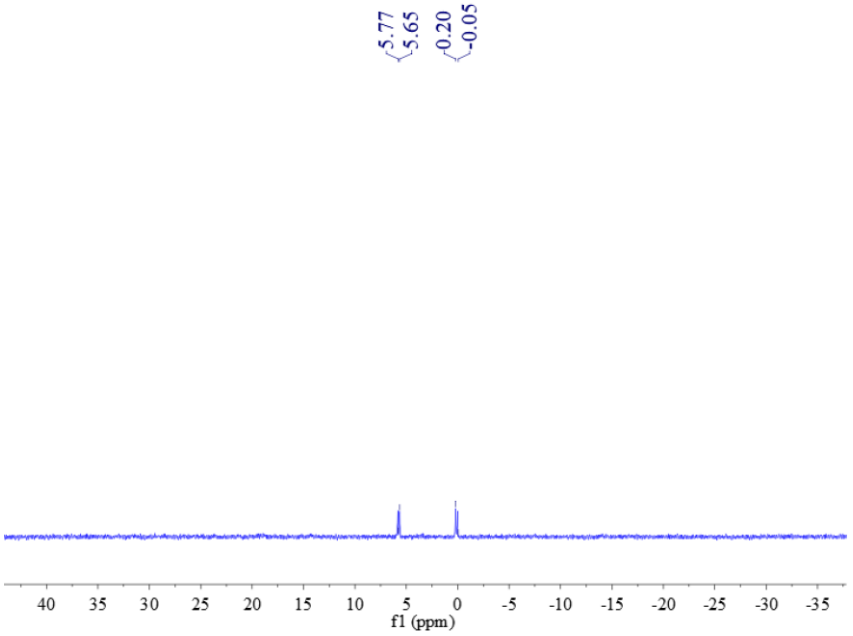

Figure S45. ^{31}P{^{1}H} NMR spectra of cage **3** based aggregates formed in THF for seven days (resuspended in DCM).

3.21 ^{31}P{^{1}H} NMR spectra of the cage 4 in THF for seven days

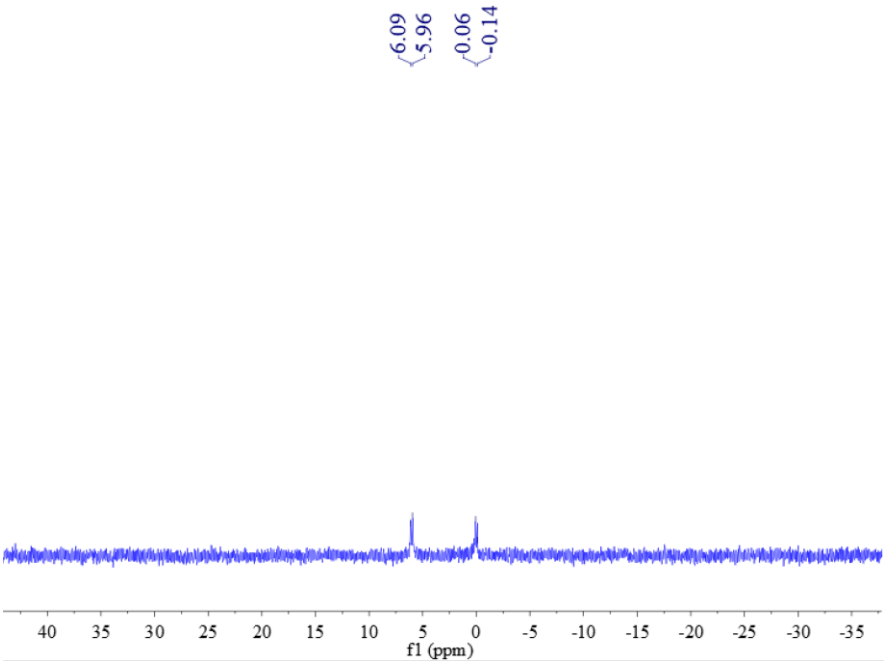

Figure S46. ^{31}P{^{1}H} NMR spectra of cage **4** based aggregates formed in THF for seven days (resuspended in DCM).